

Bipolar resistive switching characteristics in tantalum nitride-based resistive random access memory devices

Myung Ju Kim, Dong Su Jeon, Ju Hyun Park, and Tae Geun Kim

Citation: [Applied Physics Letters](#) **106**, 203101 (2015); doi: 10.1063/1.4921349

View online: <http://dx.doi.org/10.1063/1.4921349>

View Table of Contents: <http://scitation.aip.org/content/aip/journal/apl/106/20?ver=pdfcov>

Published by the [AIP Publishing](#)

Articles you may be interested in

[H-treatment impact on conductive-filament formation and stability in Ta₂O₅-based resistive-switching memory cells](#)

J. Appl. Phys. **117**, 124501 (2015); 10.1063/1.4915946

[Mechanism of the reset process in bipolar-resistance-switching Ta/TaO_x/Pt capacitors based on observation of the capacitance and resistance](#)

Appl. Phys. Lett. **104**, 123503 (2014); 10.1063/1.4869755

[Conductance quantization in oxygen-anion-migration-based resistive switching memory devices](#)

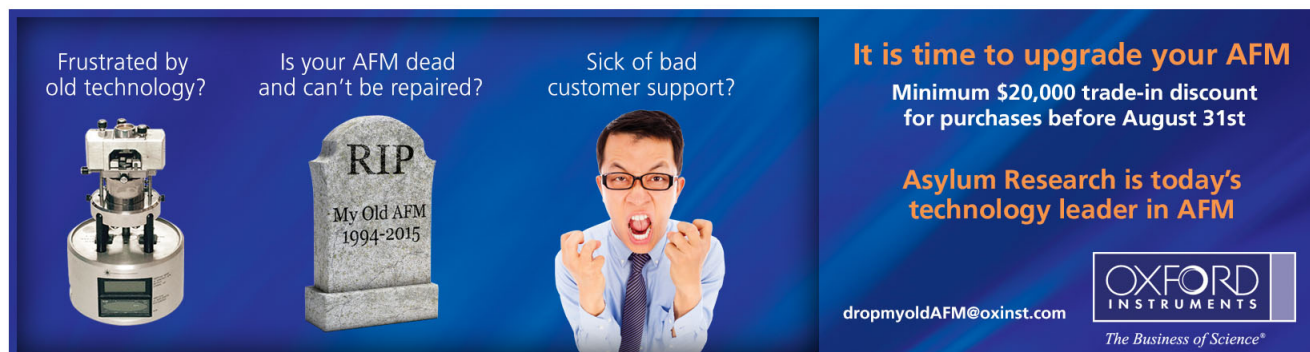
Appl. Phys. Lett. **103**, 043510 (2013); 10.1063/1.4816747

[Unipolar resistive switching behavior of Pt/Li_xZn_{1-x}O/Pt resistive random access memory devices controlled by various defect types](#)

Appl. Phys. Lett. **101**, 203501 (2012); 10.1063/1.4766725

[Switching dynamics and charge transport studies of resistive random access memory devices](#)

Appl. Phys. Lett. **101**, 113503 (2012); 10.1063/1.4749809

An advertisement for Asylum Research's AFM technology. The background is dark blue. On the left, there is a photograph of an AFM head. In the center, there is a grey tombstone with the inscription 'RIP My Old AFM 1994-2015'. To the right of the tombstone is a photograph of a man with glasses, wearing a blue shirt and tie, with a frustrated expression, his hands raised in a 'stop' gesture. Text on the left side reads: 'Frustrated by old technology?', 'Is your AFM dead and can't be repaired?', and 'Sick of bad customer support?'. On the right side, the text reads: 'It is time to upgrade your AFM', 'Minimum \$20,000 trade-in discount for purchases before August 31st', and 'Asylum Research is today's technology leader in AFM'. At the bottom right, there is a logo for 'OXFORD INSTRUMENTS' with the tagline 'The Business of Science®' and the email address 'dropmyoldAFM@oxinst.com'.

Bipolar resistive switching characteristics in tantalum nitride-based resistive random access memory devices

Myung Ju Kim, Dong Su Jeon, Ju Hyun Park, and Tae Geun Kim^{a)}

School of Electrical Engineering, Anam-dong 5ga, Sungbuk-gu, Seoul 136-701, South Korea

(Received 23 March 2015; accepted 7 May 2015; published online 18 May 2015)

This paper reports the bipolar resistive switching characteristics of TaN_x-based resistive random access memory (ReRAM). The conduction mechanism is explained by formation and rupture of conductive filaments caused by migration of nitrogen ions and vacancies; this mechanism is in good agreement with either Ohmic conduction or the Poole-Frenkel emission model. The devices exhibit that the reset voltage varies from -0.82 V to -0.62 V, whereas the set voltage ranges from 1.01 V to 1.30 V for 120 DC sweep cycles. In terms of reliability, the devices exhibit good retention ($>10^5$ s) and pulse-switching endurance ($>10^6$ cycles) properties. These results indicate that TaN_x-based ReRAM devices have a potential for future nonvolatile memory devices. © 2015 AIP Publishing LLC. [<http://dx.doi.org/10.1063/1.4921349>]

Recent semiconductor memory device technologies were required to be scaled down to achieve greater data storage. This requirement can be a significant challenge when developing conventional charge-storage-based memory devices such as nano-floating gate memory and silicon-oxide-nitride-oxide-silicon (SONOS) memory because of the technical and physical limitations of these devices.^{1–3} Resistive random access memory (ReRAM) is known to be a promising alternative because of its advanced forms such as phase-change random access memory or magnetoresistive random access memory. To further improve memory applications, resistive switching (RS) phenomena in various materials have been investigated. In particular, metal-oxide ReRAM has received much attention because of its good compatibility with semiconductor manufacturing technologies and low-cost of fabrication. Extensive research has been devoted for improving both the stability and the RS properties of these oxide materials.^{4–6} Notably, Wei *et al.* have proposed a TaO_x ReRAM device with stable resistance switching based on the redox reaction mechanism.⁷ They claim that tantalum is one of the most promising transition metals for RS operation and that the stability of the resistance state in TaO_x ReRAM is determined by the stability of the redox pair. In this case, the lower the absolute value of the Gibbs energy of the reaction, the lower the reactivity. They calculated the reaction Gibbs energy for various transition metal oxides to determine resistance change; among these, TaO_x exhibited the lowest reaction Gibbs energy. A low reaction Gibbs energy favors bistable states; therefore, it is very important from the viewpoint of reliability.⁷ Hong *et al.* have reported RS behavior using nitride-based RS materials such as aluminum nitride (AlN). These devices have features such as low voltage/current operation, fast program operation, good endurance and retention properties, and excellent compatibility with CMOS technology.^{8,9} For these reasons, it is expected that TaN_x can be used as a switching material in ReRAM applications.

In this study, we investigate the electrical properties such as the set/reset voltage distributions, low resistance

state (LRS)/high resistance state (HRS) currents of the device throughout the DC curve, RS behavior under pulsed conditions, and conduction mechanisms of a TaN_x-based device to verify its suitability in ReRAM applications.

The proposed resistive memory device was fabricated as follows. A 10-nm-thick Ti thin film and a 100-nm-thick Pt thin film were deposited as the bottom electrode on a SiO₂/p-Si (100) substrate using a radio frequency (RF) sputtering system. Then, a 50-nm-thick TaN_x thin film was deposited as a resistive switching layer at room temperature using RF magnetron sputtering. The sputtering was carried out in a mixed ambient of argon and nitrogen (Ar/O₂ gas with a flow rate of 25 sccm/10 sccm) at a power of 150 W and a working pressure of 5 mTorr. Then, the TaN_x/Pt specimens were annealed at 450 °C for 1 min in a nitrogen gas environment in a rapid thermal annealing system. Finally, a 100-nm-thick Ti top electrode was deposited on the TaN_x thin film. A schematic drawing of the fabricated ReRAM devices with Ti/TaN_x/Pt structure is presented in Fig. 1(a). To confirm the Ti/TaN_x/Pt structure, the tantalum and nitrogen elements were analyzed based on X-ray photoelectron spectroscopy (XPS) depth profiles, as shown in Fig. 1(b). In this figure, each layer was clearly identified; the ratio of Ta to N atoms was roughly 1:1 for the TaN_x layer. No diffusion from the Pt bottom electrode to the TaN_x layer was observed during the annealing process, which should predict reliable switching

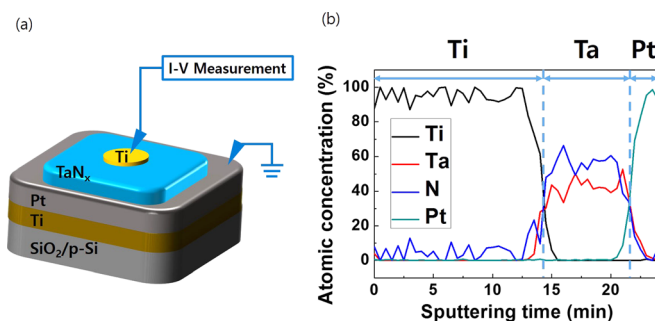


FIG. 1. (a) A schematic diagram of the Ti/TaN_x/Pt ReRAM device. (b) Atomic concentration of the four elements (i.e., Ta, N, Ti, and Pt) measured from the XPS depth profile for the Ti/TaN_x/Pt layers.

^{a)}tgkim1@korea.ac.kr

operation of the ReRAM cell. The XPS measurement was performed using a ULVAC-PHI X-TOOL. The resistive switching characteristics were measured by biasing the Ti and grounding the Pt using a Keithley 4200 semiconductor characterization system. All measurements were performed at room temperature.

Fig. 2 shows the I-V characteristics of a typical Ti/Ta_N_x/Pt ReRAM device; the device exhibits bipolar resistive switching. For all measurements, the bottom electrode was grounded and the bias was applied to the top electrode. We found that the devices were initially in the HRS for the as-deposited conditions in this work. When a positive voltage was applied to the top electrode of a device in the HRS, there was a linear increase in current on a log-linear scale, as shown in the inset of Fig. 2. At a certain voltage, roughly 1.75 V, there was a sharp increase in current as the device transitioned from the HRS to the LRS. This phenomenon is the forming process that activated the reversible RS behavior for the device; the voltage at which this transition occurs is defined as the forming voltage (V_{forming}). When a negative voltage was applied to the top electrode of a device in the LRS, resistive switching back to the HRS occurred. This transition is the reset process (device switched into the “off state”); the voltage at which this transition takes place is referred to as the reset voltage (V_{reset}). When a positive voltage was applied to the top electrode of a device in the HRS, resistive switching back to the LRS occurred. This transition is the set process (device switched into the “on state”), and the voltage at which this transition occurs is referred to as the set voltage (V_{set}). In this work, the devices usually require 1.2 V (V_{set}) to trigger resistive switching from the HRS to the LRS. In contrast, the devices switched to the HRS at approximately -0.75 V (V_{reset}). To prevent hard electrical breakdown of the devices, a compliance current was applied during the set process.^{10,11}

The statistical characteristics shown in Fig. 3 indicate that the DC cycling characteristics of the TaN_x-based ReRAM device are stable over 120 repeated positive and negative bias sweeps. Fig. 3(a) shows the distributions of the set and reset currents at 0.1 V before and after programming for the off state and on state, respectively. The currents vary

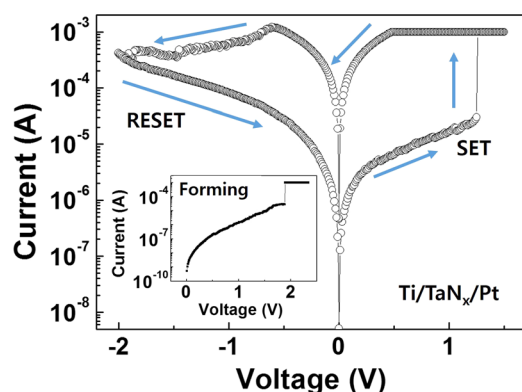


FIG. 2. Typical bipolar resistive switching characteristics for a DC voltage sweep ($0\text{ V} \rightarrow 1.5\text{ V} \rightarrow 0\text{ V} \rightarrow -1.5\text{ V} \rightarrow 0\text{ V}$) for the Ti/Ta_N_x/Pt memory cells. (Inset) Following the forming process of the device with an electrical bias ranging from 0 to 2.5 V, a sudden increase in the current is observed at around 2.0 V.

from $79.3\text{ }\mu\text{A}$ to $194.1\text{ }\mu\text{A}$ for the set state, probably because of variations in the fabrication process, whereas the distribution of the current is narrow before programming (off state). Fig. 3(b) shows the distribution of the set and reset voltages taken for 120 DC cycles for the device. The distributions of set and reset voltages are measured to be $\sim 0.29\text{ V}$ and $\sim 0.20\text{ V}$, respectively. Statistical analyses indicate that stable resistive switching occurred in the TaN_x-based ReRAM device, relative to other nitride-based ReRAM devices.^{9,12} In addition, the devices reveal the bipolar switching behavior that keeps stable on/off ratio of 8.35×10^1 with switching responses over 10^6 cycles under AC pulse biases using a pulsewidth of 50 ns and a pulse height of 2.5 V for set and -1.5 V for reset. Moreover, the data retention of more than 10^5 s at room temperature has been confirmed, as shown in Figs. 3(c) and 3(d). The on/off ratio of the device is slightly lower than those reported in the literature,¹³ but it can be improved by increasing the number of oxygen vacancies using oxygen doping, for example, as reported in Ref. 14.

To further examine the conduction mechanism of the TaN_x-based ReRAM device, the I-V curves in both the LRS and HRS regions have been replotted. To determine the current conduction mechanism in the LRS region, we have plotted $\log |I|$ vs. $\log |V|$ for the LRS, as shown in Fig. 4(a). In the low voltage region of the LRS ($V < V_{\text{reset}}$), a linear increase with a slope of roughly 1 is observed. This confirms that the conduction mechanism of the LRS is dominated by Ohmic behavior.¹⁵

To determine the current conduction mechanism in the HRS region, we examine Poole-Frenkel emission. Poole-Frenkel emission (electron conduction through traps) can be characterized by the following equation:¹⁶

$$\ln(I/V) \approx \left[\left(\frac{q^3}{\pi d \epsilon_r \epsilon_0} \right)^{\frac{1}{2}} \right] \frac{V^{\frac{1}{2}}}{k_B T},$$

where q is the electric charge, d is the thickness of film, ϵ_r is the dynamic dielectric constant, ϵ_0 is the permittivity of free space, k_B is Boltzmann's constant, and T is the absolute temperature. According to the equation for Poole-Frenkel emission, the current characteristics can be analyzed in terms of the relationship between $\ln |I/V|$ and $V^{1/2}$, which can be used to determine the dominant mechanisms.¹⁵ By replotting the data in the form of $\ln |I/V|$ vs. $|V|^{1/2}$, as shown in Fig. 4(b), the conduction mechanism can be fitted to Poole-Frenkel emission over the low-voltage region in the HRS.

According to these analysis results, a model is proposed to examine the RS behavior of the TaN_x-based ReRAM device. Previous studies have shown that the switching mechanism is dominated by nitrogen vacancy generation and recombination.^{9,12,17} As a result, we see the formation of the switching regime, including nitrogen vacancies composed of conductive filaments and the Ti reservoir. The schematic diagram in Fig. 5 shows a widely recognized device. During the set process, nitrogen atoms are removed from the lattice and nitrogen vacancies are generated, leaving vacancies behind the conductive filaments in the switching layer. Nitrogen ions drift toward the Ti interface and are stored there, forming a nitrogen reservoir. While the reset process proceeds under a

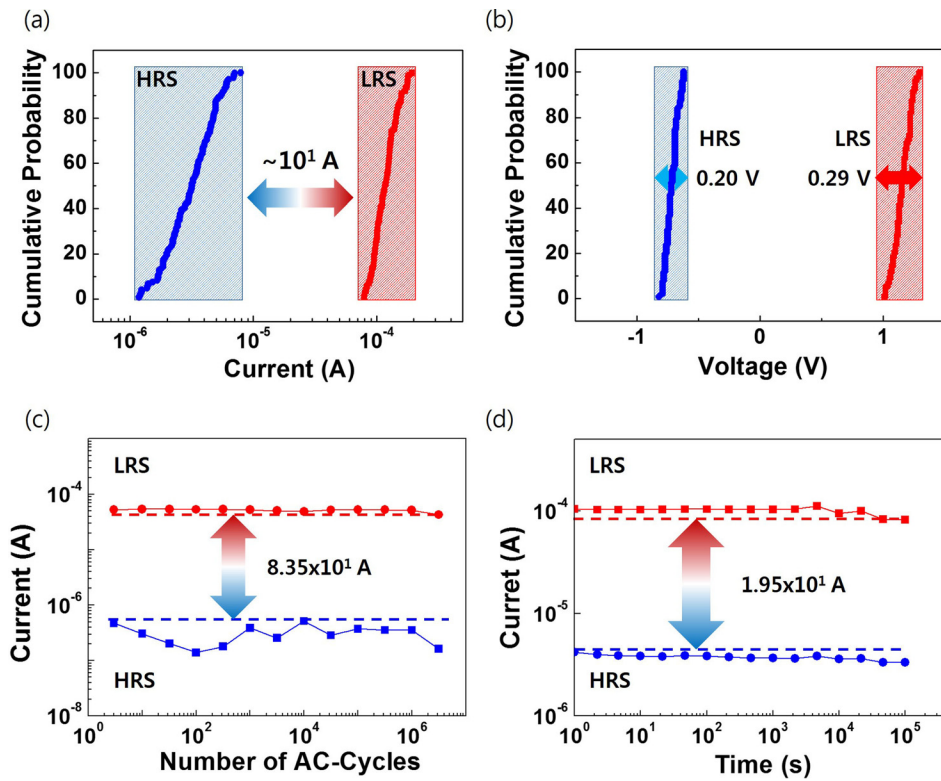


FIG. 3. I-V characteristics of a ReRAM device with the structure Ti/Ta_{N_x}/Pt. The cumulative probability of (a) current distribution and (b) voltage distribution. (c) The device shows the typical set and reset characteristics measured under AC pulse biases using a pulsewidth of 50 ns and a pulse height of 2.5 V for set and -1.5 V for reset. (d) The data retention of more than 10⁵ s at room temperature has been confirmed.

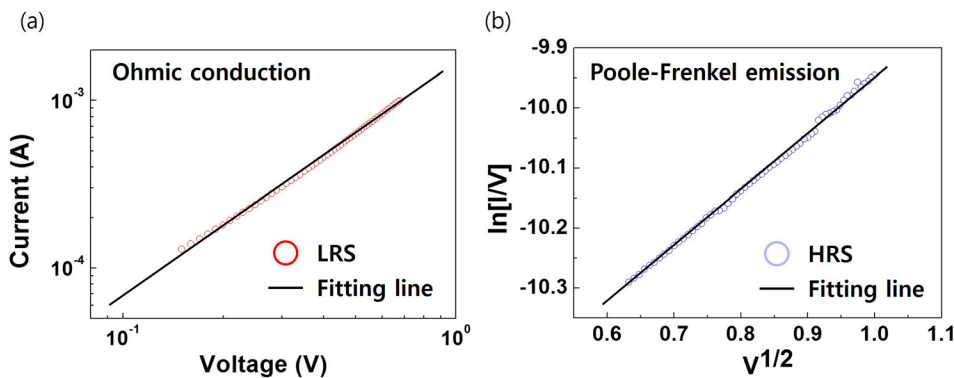


FIG. 4. Conduction mechanisms of (a) the LRS and (b) the HRS for the device. The I-V measurement data are plotted to examine Ohmic and Poole-Frenkel emission in (a) and (b), respectively.

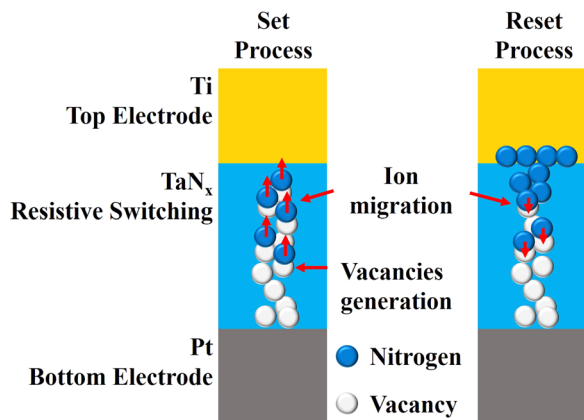


FIG. 5. Schematic diagram of the switching mechanism of Ti/Ta_{N_x}/Pt ReRAM device. The set process from HRS to LRS indicates the formation of conductive filaments via the generation of nitrogen vacancies, whereas the reset process from LRS to HRS indicates the rupture of conductive filaments via the recombination of nitrogen vacancies with nitrogen ions that migrate from the nitrogen reservoir at the Ti/Ta_{N_x} interface.

negative bias, nitrogen ions migrate from the interface back to the switching layer and recombine with vacancies, causing the rupture of conductive filaments near the Ti interface.

According to the electrical properties and the physical analysis results, the RS is thought to occur via migration of nitrogen ions between the anode and the Ta_{N_x}, as illustrated in Fig. 5. In reset operation, when applying the negative voltage to the anode, nitrogen migrates from the bulk Ta_{N_x} to the interface between the Ta_{N_x} and the Ti, which is assumed to be a nitrogen reservoir, and accumulates around the anode. Thus, the resistance state of the cell changes to the HRS. In contrast to reset operation, in set operation, when applying the positive voltage to the anode, nitrogen migrates from the interface between the Ta_{N_x} and the Ti to the bulk Ta_{N_x}; thus, the cell is switched to the LRS.

We demonstrated the bipolar RS characteristics of Ta_{N_x}-based ReRAM devices. The conduction mechanism that causes resistive switching in this material was verified to be caused by the formation and rupture of conductive

filaments via migrations of nitrogen ions and vacancies. In this case, the conduction mechanisms of LRS and HRS were dominated by Ohmic conduction behavior and Poole-Frenkel emission, respectively. When compared to the performance of metal-oxide ReRAMs reported in International Technology Roadmap for Semiconductors 2013, we found that the TaN_x-based ReRAM device exhibited stable bipolar resistive switching characteristics with very low set and reset voltages ($V_{\text{set}} = 0.84$ V and $V_{\text{reset}} = -0.75$ V) although read currents at HRS and LRS were higher ($I_{\text{read, HRS}} = 516$ nA vs. 100 pA; and $I_{\text{read, LRS}} = 43$ μ A vs. ~ 10 nA) under the same read voltage ($V_{\text{read}} = 0.1$ V).¹⁸ In addition, the narrow current and set/reset voltage distributions and the good endurance and retention properties observed in this study suggest that TaN_x thin film can be used in highly efficient ReRAM devices.

This work was supported by a government grant from the National Research Foundation of Korea (NRF) (Grant No. 2011-0028769).

- ¹J. Y. Kim, J. H. Seo, Y. W. Moon, and D. K. Choi, *Curr. Appl. Phys.* **13**(2), S30 (2013).
- ²S. C. Chen, T. C. Chang, P. T. Liu, Y. C. Wu, P. S. Lin, B. H. Tseng, J. H. Shy, S. M. Sze, C. Y. Chang, and C. H. Lien, *IEEE Electron Device Lett.* **28**(9), 809 (2007).
- ³T. C. Chen, T. C. Chang, F. Y. Jian, S. C. Chen, C. S. Lin, M. H. Lee, J. S. Chen, and C. C. Shih, *IEEE Electron Device Lett.* **30**(8), 834 (2009).
- ⁴C. Y. Dong, D. S. Shang, L. Shi, J. R. Sun, B. G. Shen, F. Zhuge, R. W. Li, and W. Chen, *Appl. Phys. Lett.* **98**(7), 072107–1 (2011).

- ⁵J. Choi, J.-S. Kim, I. Hwang, S. Hong, I.-S. Byun, S.-W. Lee, S.-O. Kang, and B. H. Park, *Appl. Phys. Lett.* **96**, 262113 (2010).
- ⁶L. Chen, Y. Xu, Q.-Q. Sun, H. Liu, J.-J. Gu, S.-J. Ding, and D. W. Zhang, *IEEE Electron Device Lett.* **31**(4), 356 (2010).
- ⁷Z. Wei, Y. Kanzawa, K. Arita, Y. Katoh, K. Kawai, S. Muraoka, S. Mitani, S. Fujii, K. Katayama, M. Iijima, T. Mikawa, T. Ninomiya, R. Miyana, Y. Kawashima, K. Tsuji, A. Himeno, T. Okada, R. Azuma, K. Shimakawa, H. Sugaya, and T. Takagi, "Highly reliable TaOx ReRAM and direct evidence of redox reaction mechanism," in *IEEE International Electron Devices Meeting*, 15–17 December 2008, pp. 1–4.
- ⁸J. Hong, D. Ho, J. Kwak, G. Chung, and M. Park, "Memory device and method of fabrication thereof, non-volatile ReRAM devices and method of fabrication thereof," South Korea Patent 0 074 034 (12 August 2008).
- ⁹H.-D. Kim, H.-M. An, E. B. Lee, and T. G. Kim, *IEEE Trans. Electron Devices* **58**(10), 3566 (2011).
- ¹⁰B. J. Choi, D. S. Jeong, S. K. Kim, C. Rohde, S. Choi, J. H. Oh, H. J. Kim, C. S. Hwang, K. Szot, R. Waser, B. Reichenberg, and S. Tiedke, *J. Appl. Phys.* **98**(3), 033715 (2005).
- ¹¹X. Cao, X. M. Li, X. D. Gao, Y. W. Zhang, X. J. Liu, Q. Wang, and L. D. Chen, *Appl. Phys. A: Mater. Sci. Process.* **97**(4), 883 (2009).
- ¹²H.-D. Kim, J. M. Yun, S. M. Hong, H.-M. An, and T. G. Kim, *J. Vac. Sci. Technol., B* **31**(4), 041205 (2013).
- ¹³Y. T. Chen, T. C. Chang, J. J. Huang, H. C. Tseng, P. C. Yang, A. K. Chu, J. B. Yang, H. C. Huang, D. S. Gan, M. J. Tsai, and S. M. Sze, *Appl. Phys. Lett.* **102**, 043508 (2013).
- ¹⁴D. S. Jeon, J. H. Park, and T. G. Kim, *J. Vac. Sci. Technol., B* **33**, 010602 (2015).
- ¹⁵S. M. Sze, *Physics of Semiconductor Devices*, 2nd ed. (Wiley, New York, 1981), p. 154.
- ¹⁶W. Y. Chang, Y. C. Lai, T. B. Wu, S. F. Wang, and F. Chen, *Appl. Phys. Lett.* **92**, 022110 (2008).
- ¹⁷Y. T. Chen, T. C. Chang, J. J. Huang, H. C. Tseng, P. C. Yang, A. K. Chu, J. B. Yang, M. J. Tsai, Y. L. Wang, and S. M. Sze, *ECS Solid State Lett.* **1**(4), P57 (2012).
- ¹⁸Semiconductor Industry Association, "International technology roadmap for semiconductors (ITRS), 2013 edition," 2014.